

Spt16 and Pob3 of *Saccharomyces cerevisiae* Form an Essential, Abundant Heterodimer That Is Nuclear, Chromatin-Associated, and Copurifies with DNA Polymerase α

Jacqueline Wittmeyer,[‡] Lisa Joss,[§] and Tim Formosa^{*†}

Departments of Biochemistry and Oncological Sciences, University of Utah, Salt Lake City, Utah 84132

Received December 3, 1998; Revised Manuscript Received April 12, 1999

ABSTRACT: Previously we showed that the yeast proteins Spt16 (Cdc68) and Pob3 are physically associated, and interact physically and genetically with the catalytic subunit of DNA polymerase α , Pol1 [Wittmeyer and Formosa (1997) *Mol. Cell. Biol.* 17, 4178–4190]. Here we show that purified Spt16 and Pob3 form a stable, abundant, elongated heterodimer and provide evidence that this is the functional form of these proteins. Genetic interactions between mutations in *SPT16* and *POB3* support the importance of the Spt16–Pob3 interaction in vivo. Spt16, Pob3, and Pol1 proteins were all found to localize to the nucleus in *S. cerevisiae*. A portion of the total cellular Spt16–Pob3 was found to be chromatin-associated, consistent with the proposed roles in modulating chromatin function. Some of the Spt16–Pob3 complex was found to copurify with the yeast DNA polymerase α /primase complex, further supporting a connection between Spt16–Pob3 and DNA replication.

DNA replication requires the coordinated activities of numerous proteins including initiation factors, single-strand DNA-binding proteins, polymerases, processivity clamps, clamp loaders, helicases, and topoisomerases (1). Protein–protein interactions are crucial for the regulation of DNA replication and its coordination with other events in the cell cycle (1, 2). To identify proteins that are involved in this process, we previously used the catalytic subunit of the essential replicative DNA polymerase α , Pol1, as an affinity ligand to chromatograph extracts of yeast cells (3). Spt16 and Pob3 were identified using this technique, and the results from subsequent co-immunoprecipitation and genetic experiments supported the formation of complexes containing Pol1, Spt16, and Pob3 in vivo (3).

SPT16 was previously identified by several groups as a global regulator of transcription (4–6). Cells containing a mutation in *SPT16* (*cdc68-1*) arrest with an unbudded morphology at the nonpermissive temperature, and display aberrant transcription of several genes (4). *SPT16* was also found in a screen to identify factors that play a general role in transcriptional regulation as a suppressor of *Ty* insertion mutations in *HIS4* and *LYS2* (5). *SPT16* was classified as a member of the histone-like group of *spt* mutants because of the phenotypic similarities with mutations in *SPT11* (*HTA1*) and *SPT12* (*HTB1*), which encode histones H2A and H2B, respectively (5). Because of this phenotypic similarity with mutations in histones and the pleiotropic effects that *spt16* mutations confer on the transcriptional regulation of genes, Spt16 has been postulated to regulate the properties of chromatin (4, 5, 7–9).

POB3 (Polymerase one-binding) shares significant sequence similarity with an HMG1-like protein found in a variety of organisms, including human SSRP1 (3). *SPT16* and *POB3* are each essential for viability (3, 5); and both Spt16 and Pob3 are highly conserved among a broad range of eukaryotes (3, 10).

Recently, a complex called DUF (DNA unwinding factor) consisting of 140 and 87 kDa proteins that share significant sequence similarity with *S. cerevisiae* Spt16 and Pob3 proteins was purified from *Xenopus* egg extracts (11). Immunodepletion of DUF from these extracts diminished their ability to replicate exogenously added sperm nuclei or plasmid DNA, suggesting a role for this complex in DNA replication. This is consistent with our previous observation of physical and genetic interactions between Spt16–Pob3 and replication proteins (3, 12).

We report here that the *S. cerevisiae* Spt16 and Pob3 proteins form a stable, abundant complex, most or all of the Spt16 and Pob3 proteins in the cell are found in these complexes, and both components localize to the nucleus. A portion of the Spt16–Pob3 is chromatin-associated and Spt16–Pob3 can be detected copurifying with DNA polymerase α . Our data, taken together with previous data implicating Spt16 and Pob3 as modulators of chromatin structure, suggest that DNA polymerase α may interact with the Spt16–Pob3 complex to allow the replication machinery to access or progress through chromatin templates.

EXPERIMENTAL PROCEDURES

Media and Strains. Synthetic medium (13), YEPD (13), and YM-1 (14) were prepared as described previously. All strains used are congenic with A364a, except JSY1238.

Size-Exclusion Chromatography on Whole Cell Lysates. Cultures (2 L) of the protease-deficient strain 7382-3-4

* Corresponding author. Phone: 801-581-5435. Fax: 801-581-7959. E-mail: formosa@medschool.med.utah.edu.

[‡] Department of Biochemistry.

[§] Department of Oncological Sciences.

(*MATa leu2 ura3 trp1 his7 can1 pep4 prb1*) were grown to an $OD_{600} = 1$ in YM-1, collected by centrifugation at 3000g for 5 min, frozen in liquid nitrogen, and stored at -70°C . Cells were lysed in an equal volume of lysis buffer consisting of 20 mM Tris·HCl, pH 7.5, 200 mM NaCl, 1 mM EDTA, 1 mM 2-mercaptoethanol, 10% glycerol (w/v), 0.7 $\mu\text{g/mL}$ leupeptin, 0.5 mM phenylmethylsulfonylfluoride (PMSF), and 0.5 $\mu\text{g/mL}$ pepstatin. An equal volume of acid-washed glass beads (425–600 μm ; Sigma) was added to the cell slurry, and the cells were sheared with 10 1 min pulses on a vortexer. The supernatant was removed, and the glass beads were washed several times with lysis buffer. The lysate was cleared by centrifugation at 13000g for 10 min, then at 200000g for 2 h at 4°C . The supernatant was filtered through 0.45 and 0.2 μm cellulose–acetate syringe filters. The cleared lysate was loaded directly onto a Sephacryl S300 column (16 mm \times 60 cm, Pharmacia). Chromatography was performed in lysis buffer containing 200 mM NaCl. Column fractions were analyzed by SDS–PAGE (15) followed by immunoblotting using the polyclonal antisera raised against Spt16 or Pob3 (described below) and developed colorimetrically as described previously (3). Molecular mass standards including thyroglobulin (670 kDa), apoferritin (440 kDa), catalase (232 kDa), aldolase (158 kDa), and bovine serum albumin (67 kDa) were fractionated on the Sephacryl S300 column under the same conditions in separate experiments to calibrate the matrix.

Overexpression and Purification of Spt16 and Pob3. The *GAL1-SPT16* overexpression plasmid pJW22 was constructed by subcloning a *Bam*HI fragment containing the *SPT16* open reading frame (ORF) from pJW9 (3) into the *Bam*HI site of pJS227 (which contains a *GAL1* promoter fragment in YEplac195, *URA3*) (16). pJW22 complements the temperature-sensitivity of *cdc68-1* strains in the presence of galactose, but not glucose. The *GAL1-POB3* overexpression plasmid pJW21 was constructed by inserting the *Dra*I–*Hind*III fragment from cosmid 9745 (ATCC) containing the majority of the *POB3* ORF, along with an *Nco*I–*Dra*I PCR product that reconstructs the 5'-end of the *POB3* ORF, into the *Nco*I–*Hind*III sites of pMTL (*GAL1-YCpLEU2*) (17). The integrity of the PCR product was confirmed by DNA sequencing. The final protein product consists of full-length Pob3 with two additional residues (Met-Ala-) at the amino terminus. pJW21 complements a *pob3* Δ deletion in the presence of galactose, but not glucose.

pJW21 and pJW22 were introduced into the protease-deficient strain 7382-3-4 (*MATa leu2 ura3 trp1 his7 can1 pep4 prb1*) and maintained under selection. Spt16 and Pob3 were overexpressed simultaneously by growing this strain in media containing 3% glycerol, 2% lactate to an $OD_{600} = 0.2$ – 0.5 , and then inducing the expression of both proteins overnight with the addition of 0.5% galactose. Cells were harvested at $OD_{600} = 0.5$ – 1.4 by centrifugation at 3000g for 10 min, frozen in liquid nitrogen, and stored at -70°C .

These cells (73 g from 20 L) were lysed and cleared as described above except that the lysis buffer contained 100 mM NaCl, 1.5 volumes of acid-washed glass beads were added, and the beads were sheared with 15 2 min pulses in an ice-packed cell beater (Bio-spec Products).

A DEAE-cellulose (60 mL DE52, Whatman) column was loaded with 50 mL of cleared lysate, washed with at least 4 column volumes of lysis buffer containing 200 mM NaCl,

and then eluted with a linear gradient of 200–300 mM NaCl in lysis buffer. Spt16 and Pob3 were detected by Coomassie blue staining of SDS–polyacrylamide gels and/or immunoblotting as described previously (3). Fractions were pooled and loaded onto a hydroxylapatite (20 mL HAP, BioRad HTP) column that had been preequilibrated with HAP buffer containing 100 mM potassium phosphate, pH 7.8, 200 mM NaCl, 10% glycerol (w/v), 1 mM EDTA, 1 mM 2-mercaptoethanol, 0.7 $\mu\text{g/mL}$ leupeptin, 0.5 mM PMSF, and 0.5 $\mu\text{g/mL}$ pepstatin. The column was then washed with 2–3 column volumes of HAP buffer containing 150 mM potassium phosphate and eluted with a gradient of 150–400 mM potassium phosphate in HAP buffer. Fractions containing Spt16–Pob3 were pooled, ammonium sulfate and sodium phosphate (pH 7) were added to 1 M and 50 mM, respectively, and the sample was loaded onto a Phenylsuperose column (8 mL, Pharmacia). The Spt16–Pob3 complex flowed through this column, whereas excess free Spt16 was retained under these conditions. Using a Centriprep-10 (Amicon), the flow-through was concentrated and the buffer exchanged to size-exclusion buffer containing 20 mM Tris·HCl, pH 7.5, 200 mM NaCl, 10% glycerol (w/v), and 1 mM 2-mercaptoethanol. The Spt16–Pob3 complex was then fractionated on a Superdex 200 (26 mm \times 60 cm, Pharmacia) size-exclusion column and concentrated using a Centriprep-10. The yield of purified Spt16–Pob3 was 1.5 mg from 73 g of cells.

Production and Purification of Antisera. The purified Spt16–Pob3 complex was separated by SDS–PAGE and briefly stained with Coomassie blue. Bands corresponding to Spt16 and Pob3 were excised and individually injected into rabbits for the production of polyclonal antisera by CoVance Research Products.

For immunofluorescence, IgG was purified from the whole serum using hydroxylapatite chromatography as described (18). This procedure diluted the serum 10-fold. Affinity-purified antibodies were obtained by incubating the IgG with strips of nitrocellulose containing purified Spt16 for 1.5 h at room temperature, washing the strips several times with phosphate-buffered saline (PBS: 115 mM NaCl, 16 mM sodium phosphate, 4 mM potassium phosphate, pH 7.3), and eluting the bound antibodies by incubation in 0.2 M glycine, pH 2.8, for 2 min followed by rapid neutralization with Tris·HCl. Each antibody fraction was preadsorbed to fixed, undigested cells for 1–2 h at 4°C to remove any cross-reactivity to residual cell wall components.

Equilibrium Sedimentation. The buffer of the Spt16–Pob3 complex was exchanged by passage over a Bio-spin P-30 column (BioRad) that was preequilibrated in 20 mM Tris·HCl, pH 7.5, and 200 mM NaCl. Protein samples were centrifuged at 20°C in a Beckman XL-A at 10 000 or 13 000 rpm until sedimentation and chemical equilibrium were attained. Data analysis was performed using the NONLIN program (19). Analysis of data from the analytical ultracentrifuge was performed using nonlinear least-squares techniques (19).

Complex Abundance. The concentration of the purified Spt16–Pob3 complex was determined using the absorbance at 280 nm and the calculated extinction coefficient ($\epsilon_{1\text{mg/mL}} = 0.85$) determined as described (20). A culture of the protease-deficient strain 7382-3-4 (*MATa leu2 ura3 trp1 his7 can1 pep4 prb1*) was grown to an $OD_{600} = 0.3$ – 0.8 in YM-1

and sonicated for 5 s, and the cells were counted using a hemacytometer. The standards and cells were boiled in SDS sample buffer, separated by SDS–PAGE, and immunoblotted as described above. The signals from the immunoblots were quantitated using Scion Image 1.59 software. The whole cell signals were within the linear response range for both proteins.

Indirect Immunofluorescence. Cultures of strain JSY1238 (*MATa leu2Δ1, ura3-52, his3Δ200*) were grown to an $OD_{600} = 0.9$, fixed in 4% formaldehyde at 30 °C for 30 min, washed twice in 1.2 M sorbitol and 0.1 M potassium phosphate, pH 7.5, and incubated in sorbitol buffer containing 28 mM 2-mercaptoethanol and 0.4 mg/mL zymolyase (100T, ICN) at 37 °C for 30 min. Cells were either used directly or washed twice with sorbitol buffer and stored at 4 °C.

Teflon-coated slides (Polyscience) were prepared by coating with 1 mg/mL poly-L-lysine for 1 min, rinsing several times with water, and dried. An aliquot of the cell slurry was applied to each well, allowed to settle, washed several times with 0.5% bovine serum albumin (BSA) in PBS, and incubated for 30 min in the same solution. Affinity-purified antibodies were used for Spt16 at a dilution of 1:10, and IgG-purified fractions were used for Pob3 and Pol1 at dilutions of 1:10 and 1:200, respectively. Cells were incubated with the primary antibodies overnight at 4 °C, washed extensively with 0.5% BSA in PBS, incubated with FITC-conjugated goat anti-rabbit antibody (Jackson Laboratory) at a 1:200 dilution for 1–2 h at room temperature, and washed extensively with 0.5% BSA in PBS. A drop of mounting medium (21) containing the DNA-specific dye DAPI (4',6-diamidino-2-phenylindole dihydrochloride) was added to each well, and the cells were visualized using a Zeiss Axioplan microscope (1.25× optivar setting). Images were captured using a Hamamatsu C5810 Color Chilled 3CCD camera (Hamamatsu Photonics, Hamamatsu-City, Japan) interfaced to a Macintosh Quadra 840AV computer.

Chromatin Fractionation. A chromatin fraction was prepared essentially as described (22). Briefly, spheroplasts were prepared from a culture of protease-deficient strain 7382-3-4 (*MATa leu2 ura3 trp1 his7 can1 pep4 prb1*) harvested at an $OD_{600} = 1$, lysed in extraction buffer (50 mM HEPES–KOH, pH 7.5, 100 mM KCl, 2.5 mM $MgCl_2$, 50 mM NaF, 5 mM NaP_2O_7 , 0.1 mM Na_3VO_4 , 0.5% Triton X-100, 0.7 μ g/mL leupeptin, 0.5 mM PMSF, 0.5 μ g/mL pepstatin, and 0.2 mg/mL bacitracin), and centrifuged at 16000g for 10 min. The pellet was washed with an equal volume of extraction buffer, respun, and resuspended in an equal volume of extraction buffer (0.25% Triton X-100) containing 1 mM $CaCl_2$. The resuspended pellet was divided into two aliquots, and each was incubated for 2 min at 37 °C, followed by the addition of either buffer alone (20 mM Tris·HCl, pH 8.0, 1 mM $MgCl_2$, and 1 mM $CaCl_2$) or this buffer containing micrococcal nuclease (10 units/mL, Worthington Biochemicals) and incubated for 2 min at 37 °C. Reactions were quenched by the addition of EGTA to 1 mM. After centrifugation of the samples at 8200g for 2 min, the resulting supernatant was then centrifuged at 100000g for 1 h. The high-speed pellet was resuspended in a volume of extraction buffer equal to that of the high-speed supernatant. Samples were boiled in SDS sample buffer, separated by SDS–PAGE, and either stained with Coomassie blue or transferred to nitrocellulose and immunoblotted with anti-Spt16, anti-

Pob3, or anti-histone H3 (N-terminal peptide, Upstate Biotechnology) antisera.

Overexpression and Purification of DNA Polymerase α . *POL1* and *PRI2* were placed under control of a *GAL1*,10 promoter fragment in YEplac195 (16) using the *POL1* *Bam*HI fragment previously described (23) and a *PRI2* PCR product. PCR products of *POL12* and *PRI1* were similarly inserted into a YEplac181 derivative (16). This yielded two high-copy plasmids (pTF132 and pTF136) with different selectable markers that overexpress the four subunits of DNA polymerase α in response to galactose. Each of the PCR products was confirmed by DNA sequencing, and each produces a protein with the same sequence as the normal A364a genetic background.

pTF132 and pTF136 were transformed into the protease-deficient strain 7382-3-4 (*MATa leu2 ura3 trp1 his7 can1 pep4 prb1*) and maintained under selection. Pol1, Pol12, Pri2, and Pri1 were overexpressed simultaneously by growing this strain in media containing 3% glycerol, 2% lactate to an $OD_{600} = 0.4$ –0.6, then inducing the expression of the four proteins over 20–40 h with the addition of 0.5% galactose. Cells were harvested at $OD_{600} = 1.0$ or above by centrifugation at 3000g for 10 min, frozen in liquid nitrogen, and stored at –70 °C.

These cells (140 g from 30 L) were lysed and cleared as described above for the purification of Spt16–Pob3 with the following exceptions. The lysis buffer consisted of 0.2 M Tris·HCl, pH 7.5, 20 mM potassium acetate, 2 mM EDTA, 2 mM 2-mercaptoethanol, 0.2% Triton X-100, 20% glycerol (w/v), 0.7 μ g/mL leupeptin, and 0.5 μ g/mL pepstatin. The low-speed lysate was precipitated with 60% saturated ammonium sulfate for 30 min at 4 °C and centrifuged at 16000g for 10 min, and the pellet was resuspended in an equal volume of PC₁₀₀ buffer (100 mM potassium phosphate, pH 7.8, 100 mM NaCl, 1 mM EDTA, 1 mM 2-mercaptoethanol, 10% glycerol, 0.7 μ g/mL leupeptin, and 0.5 μ g/mL pepstatin) and dialyzed twice against 4 L of PC₁₀₀ buffer. The dialysate was then spun at 200000g for 2 h at 4 °C and filtered through 0.45 and 0.2 μ m cellulose–acetate syringe filters.

A phosphocellulose (150 mL, Whatman P11) column was loaded with 250 mL of the cleared dialysate, washed with at least 4 column volumes of PC₁₀₀ buffer, and then eluted with a gradient of PC₁₀₀ buffer containing 100–450 mM NaCl. Fractions were monitored by Coomassie blue staining of SDS–polyacrylamide gels and/or immunoblotting using anti-Pol1 antiserum. Fractions containing the Pol α complex were pooled and loaded onto a hydroxylapatite (10 mL HAP, BioRad HTP) column that had been preequilibrated with PC₁₀₀ buffer and eluted with a gradient of 100–400 mM potassium phosphate in PC₁₀₀ buffer. Fractions containing Pol α were pooled, concentrated using a Centriprep-10 (Amicon), fractionated on a Sephacryl S300 (16 mm × 60 cm, Pharmacia) size-exclusion column in buffer consisting of 20 mM Tris·HCl, pH 7.5, 100 mM NaCl, 1 mM EDTA, 1 mM $MgCl_2$, 10% glycerol (w/v), and 1 mM 2-mercaptoethanol, and then concentrated using a Centriprep-10 (Amicon). The yield of purified Pol α complex was 4.4 mg from 140 g of cells.

POB3 Mutagenesis. pJW4 and pJW11 were constructed by cloning the 3.9 kb *KpnI*–*SphI* fragment containing the *POB3* gene from cosmid 9745 (ATCC) into the same sites of YCplac33 (*CEN, URA3*) and YCplac111 (*CEN, LEU2*),

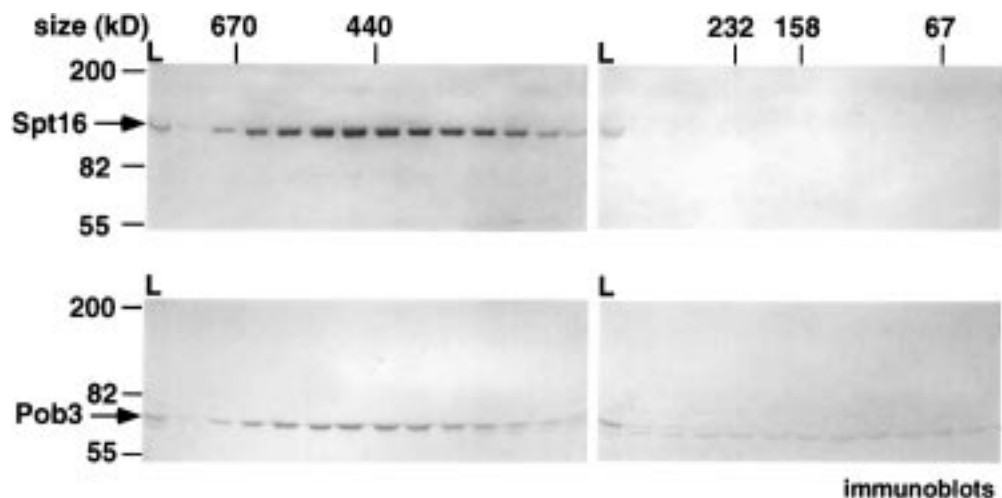


FIGURE 1: Size-exclusion chromatography of Spt16 and Pob3 from whole cell lysates. A whole cell lysate prepared from wild-type cells was chromatographed on a Sephacryl S300 column, and fractions were analyzed on immunoblots using antisera directed against Spt16 or Pob3. The molecular masses listed at the top of each panel reflect the elution of standards from the same column, and those at the left reflect the migration of SDS-PAGE standards. (L) Lysate loaded onto the column. The asterisk (*) indicates a protein in whole cell lysates that cross-reacts with the anti-Pob3 antisera, but is not Pob3 based on the following: the levels of this protein do not change when Pob3 is overexpressed, and this protein flows through a DEAE column whereas Pob3 binds to this resin in 100 mM NaCl buffer.

respectively (16). pJW11 was mutagenized with hydroxylamine essentially as described (24). The mutagenized pJW11 was exchanged in a plasmid shuffle for pJW4 in strain 7697, and isolates were assayed for both temperature- and cold-sensitivity. Of 30 000 isolates that were screened, 3 plasmid-linked alleles were found to confer temperature-sensitivity.

Temperature-Sensitivity Analysis. Strains 7697/pJW4 [*MATa trp1 leu2 ura3 his7 pob3-Δ5::TRP1* pJW4 (*POB3, URA3*)], 7697/pJW11-x [*MATa trp1 leu2 ura3 his7 pob3-Δ5::TRP1* pJW11-x (*pob3-x, LEU2*)], 7399-3-1 [*MATa trp1 leu2 ura3 his3*], 2034-3-2 [*MATa trp1 leu2 ura3 his3 spt16 (cdc68-1)::URA3*], 7732-1-4 [*MATa trp1 leu2 ura3 his3 spt16 (cdc68-1)::URA3 pob3-Δ5::TRP1* pJW11-10], 7732-1-1 [*MATa trp1 leu2 ura3 his3 spt16 (cdc68-1)::URA3 pob3-Δ5::TRP1* pJW11-11], and 7732-3-1 [*MATa trp1 leu2 ura3 his3 spt16 (cdc68-1)::URA3 pob3-Δ5::TRP1* pJW11-12] were grown to saturation in YM-1, diluted 100-fold serially, spotted onto YEPD plates, and incubated at the indicated temperatures for 4 days.

Acetyltransferase Assay. Purified Spt16–Pob3 complex or Hat1 (1 μg of each) was incubated in a buffer consisting of 65 mM Tris·HCl, pH 8.8, 130 mM NaCl, 0.3 mM EDTA, 9 μM [³H]acetyl-coenzyme A (1.9 Ci/mmol, NEN), and 0.05 mg/mL purified core histones (from chicken erythrocytes, a generous gift from Venki Ramakrishnan) in a 20 μL reaction for 30 min at 37 °C. Reactions were quenched by the addition of SDS sample buffer, boiled, fractionated by SDS-PAGE, and stained with Coomassie blue. The stained gel was incubated in Enhance (NEN) for 1 h, then 10% poly(ethylene glycol) 8000 for 1 h, dried, and exposed to film overnight.

RESULTS

Spt16 and Pob3 Form a Complex. Three lines of evidence previously suggested that Spt16 and Pob3 form a complex: (1) in the absence of another Pol1-binding protein, Ctf4, the binding of both Spt16 and Pob3 to a Pol1 affinity matrix increased in approximately stoichiometric levels (3); (2) Pob3 co-immunoprecipitated with Spt16 (3, 25); and (3) when either Spt16 or Pob3 was overexpressed, the other protein

coeluted from both anion exchange and hydroxylapatite columns (our unpublished results).

To determine the size of the endogenous Spt16 and Pob3 complex, we performed size-exclusion chromatography on whole cell lysates followed by immunoblot analysis of the fractions. Spt16 (118.5 kDa) and Pob3 (63 kDa) coeluted in the 400–500 kDa range (Figure 1), whereas a heterodimer of these proteins should have a mass of 181 kDa. Thus, either the complex may contain additional proteins besides Spt16 and Pob3, it may contain multiple protomers of Spt16 and Pob3, or it might be a heterodimer of Spt16–Pob3 that has an elongated shape. Furthermore, there is no evidence for a monomer of either Spt16 (25) or Pob3 in whole cell lysates (Figure 1), suggesting the complex is the functional, biologically relevant form of both proteins, although we cannot rule out the possibility of an additional less stably associated small subunit.

Spt16 and Pob3 Copurify. Spt16 and Pob3 were overexpressed in the same cells to determine whether this would result in the overexpression of a stable complex. Overexpressed Spt16 and Pob3 copurified through four purification steps, including anion exchange, hydroxylapatite, hydrophobic affinity, and size-exclusion chromatography (Figure 2). The overexpressed, purified complex eluted from the size-exclusion column in the same range (400–500 kDa) as the endogenous Spt16 and Pob3 from whole cell lysates (Figure 1 and data not shown). The Spt16–Pob3 complex that was purified from cells expressing normal levels of each protein also eluted in this same size range (400–500 kDa, data not shown), so this profile is not an artifact of overexpression. The copurification of Spt16 and Pob3 through several chromatographic steps indicates that these proteins form a complex that is stable under a variety of conditions. The absence of other proteins in the purified endogenous complex and the similar chromatographic behavior of the endogenous and overexpressed purified complexes indicate that the anomalous behavior in size-exclusion matrixes is likely to result from the complex either containing multiple protomers of these proteins or having an elongated shape.

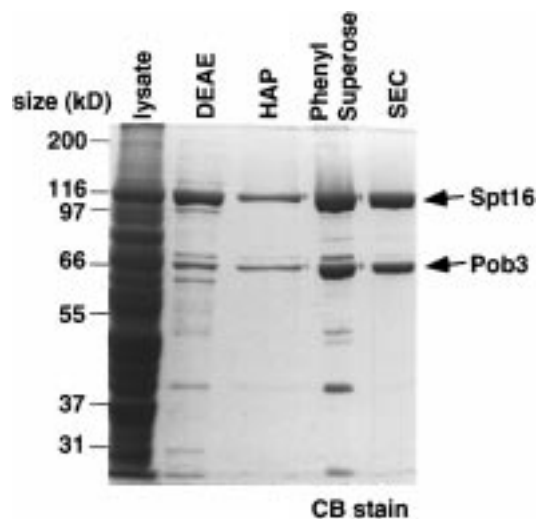


FIGURE 2: Overexpression and purification of the Spt16–Pob3 complex. Aliquots of the whole cell lysate and the eluates from the DEAE, hydroxylapatite (HAP), phenylsuperose, and size-exclusion chromatography (SEC) matrixes were separated by SDS–PAGE and stained with Coomassie blue. Immunoblot analysis revealed that the two minor proteins in the final preparation which migrate between Spt16 and Pob3 are degradation products of Spt16 (not shown).

The Spt16–Pob3 Complex Is a Stable, Elongated Heterodimer. To determine the oligomeric composition of the Spt16–Pob3 complex, we examined the overexpressed, purified complex by analytical ultracentrifugation. Equilibrium sedimentation is a shape-independent technique that can be used to accurately determine the size of a macromolecule in solution, and therefore can provide the subunit stoichiometry of two proteins within a complex.

Prior to conducting the equilibrium sedimentation experiment, a velocity sedimentation experiment was performed to determine whether all of the Spt16 and Pob3 molecules were participating in the formation of a complex (i.e., to assess whether any of the protomers were misfolded and unable to associate with their partner) and, therefore, to assess whether the results of the equilibrium sedimentation experiment would be interpretable. The results from the velocity sedimentation experiment (data not shown) indicated that all of the Spt16 and Pob3 molecules were indeed participating in the formation of a complex and that the complex appeared to be stable. Some information about the shape of the protein can be derived from this analysis by examining a shape factor ($F = f/f_0$) which normalizes the frictional coefficient obtained from sedimentation velocity (f) to that of a sphere (f_0) of the same molecular weight. A value of F greater than unity suggests that the protein deviates from a spherical shape. The degree of deviation can be correlated with the axial ratio of an ellipsoid in order to estimate the true shape of the molecule. In the case of the Spt16–Pob3 complex, the shape factor was approximately 1.6. This is consistent with a molecular shape corresponding to a prolate ellipsoid (rodlike) with one axis being 12-fold longer than the other two, or an oblate ellipsoid (disklike) with two axes being 15-fold longer than the third. These data, as well as the data from the size-exclusion chromatography, are consistent with the Spt16–Pob3 complex having an elongated shape.

The equilibrium sedimentation data (Figure 3) were best described by a model of a single nonideal species with a

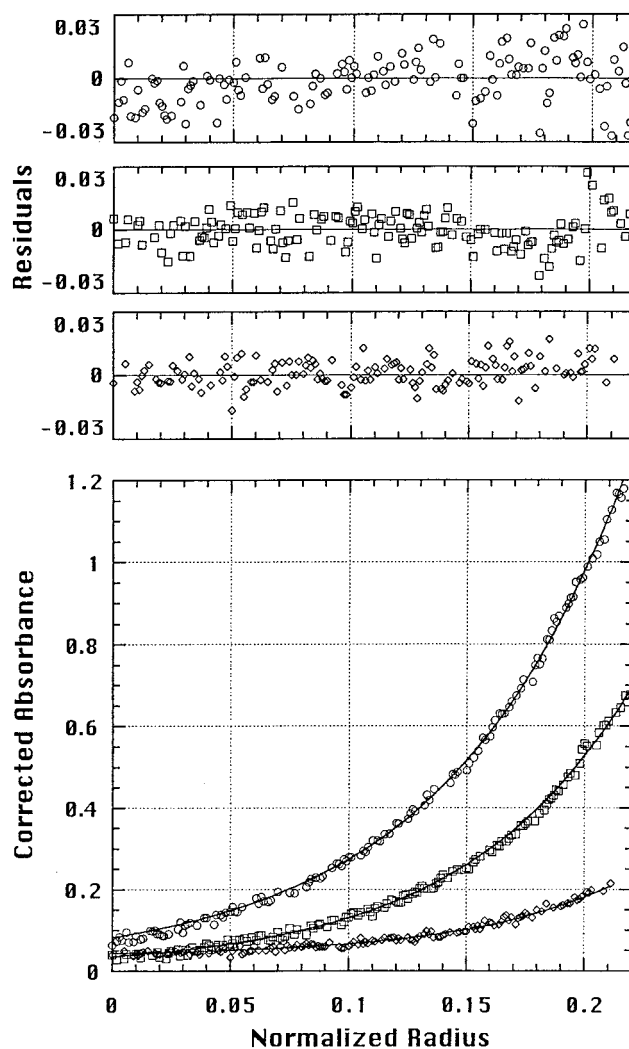


FIGURE 3: Equilibrium sedimentation. The lower panel shows the fit (solid line) of a single nonideal species model to six experimental data sets that were fit simultaneously [for clarity, we show only three initial loading concentrations represented as (circles) 0.5 mg/mL, (squares) 0.25 mg/mL, and (diamonds) 0.016 mg/mL]. Data were collected at 280 or 230 nm and then corrected for stray light and window aberrations by subtraction of a scan taken at 340 nm. The upper panels show the residuals for the fits.

molecular mass of 176 kDa (± 10 kDa), consistent with a predicted mass of 181 kDa for a heterodimer of Spt16–Pob3 (which is therefore stable for at least 36 h at 20 °C). The second virial coefficient, which is a measure of nonideality, is represented by a value of $0.26 \times 10^{-6} \text{ mol} \cdot \text{L}^{-1} \cdot \text{g}^{-2}$. This nonideal behavior likely results from steric interactions produced as a result of an elongated shape. The final fit simultaneously incorporated six different concentration distributions obtained from initial loading concentrations ranging from 0.5 to 0.016 mg/mL and data collected at 280 or 230 nm. The fit and residuals for three of these data sets are shown in Figure 3. The fitting strategy initially allowed the molecular weight and base line offset values to float; then after satisfactory convergence, the second virial coefficient was also floated, thereby significantly improving the fit. Overall, the fits were good, as indicated by small sums of squares and small, randomly distributed residuals. This experiment was repeated at a second speed (13 000 rpm) with comparable results. The analytical centrifugation and size-exclusion chromatography data are consistent with the

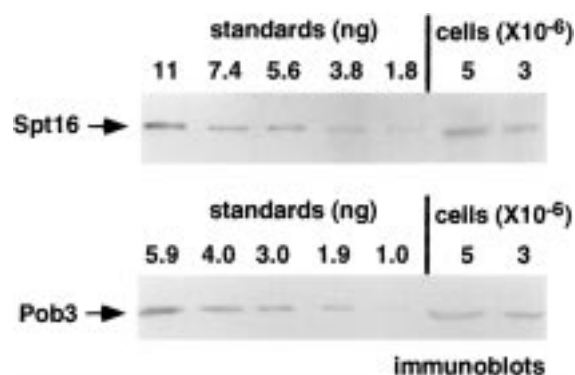


FIGURE 4: Abundance of the Spt16–Pob3 complex. Known quantities of purified Spt16–Pob3 complex (standards) and defined numbers of cells were boiled in SDS sample buffer, separated by SDS–PAGE, and analyzed on immunoblots with antibodies against Spt16 and Pob3. The bands were quantitated using Scion Image 1.59. This is a representative example of at least three experiments.

Spt16–Pob3 complex being a stable, elongated heterodimer.

The Spt16–Pob3 Complex Is Abundant. To determine the relative abundance of Spt16 and Pob3 in the cell, we correlated the intensity of bands on immunoblots corresponding to Spt16 and Pob3 from a known number of cells with those from specific quantities of purified complex. There were approximately 2.3 ng of Spt16 and 0.9 ng of Pob3 per million cells (Figure 4). Assuming a molecular weight of 118 500 for Spt16 and 63 000 for Pob3, we estimate that there are $\sim 10\,000$ copies of the Spt16–Pob3 complex per haploid cell. We repeated this analysis of copy number at least 3 times for both proteins and found our results to be reproducible within a factor of 2. Our results differ from those in another study in which Spt16 was reported to be 50 000 copies per cell (25). In that study, bacterially expressed Spt16 was purified and quantified using methods subtly different from those used here, which may account for some of the discrepancy.

Spt16, Pob3, and Pol1 localize to the nucleus in *S. cerevisiae*. To determine the intracellular localization of the

protein components of this complex, we used indirect immunofluorescence. Polyclonal antisera directed against either Spt16 or Pob3 revealed both to be nuclear proteins, whereas the preimmune controls lacked signal (Figure 5). This is consistent with a previous study that reported HA-tagged Spt16 to be nuclear (9) and our observation that Spt16 and Pob3 always form a complex (Figure 1). Pol1 was also localized to the nucleus in *S. cerevisiae* (Figure 5), consistent with observations in *Schizosaccharomyces pombe* (26) and mammalian cells (27–29). Furthermore, we did not observe any cell cycle dependent changes in the nuclear localization of Spt16, Pob3, or Pol1.

A Portion of Spt16–Pob3 Is Chromatin-Associated. Previous genetic analysis of *SPT16* and the sequence similarity of Pob3 with HMG1-like proteins suggested that the Spt16–Pob3 complex may modulate chromatin structure. To determine whether these proteins are components of chromatin, we prepared chromatin from a rapidly growing culture of wild-type cells and monitored the distribution of Spt16 and Pob3 during the fractionation.

Spheroplasts were lysed and centrifuged at low speed to separate the soluble and insoluble fractions (Figure 6A); the latter includes chromatin as well as other subcellular components. The majority ($\sim 75\%$) of the Spt16–Pob3 was soluble (data not shown), but some was found in the insoluble fraction even after a brief wash (Figure 6B, fraction 1). Partial digestion of chromatin with micrococcal nuclease releases poly-nucleosomal fragments that can subsequently be pelleted by centrifugation at 100000g, but not at 8200g (22). Nuclease treatment should not affect the solubility of other non-chromatin material. Therefore, the enrichment of a factor in the 100000g pellet following micrococcal nuclease treatment provides evidence for its association with chromatin. When the washed, low-speed pellet (Figure 6A,B, fraction 1) was subjected to partial nuclease digestion, a portion of the Spt16 and Pob3 was converted into a form that was soluble during a low-speed centrifugation step (Figure 6B, fraction 2), but was then pelleted during a subsequent high-speed centrifuga-

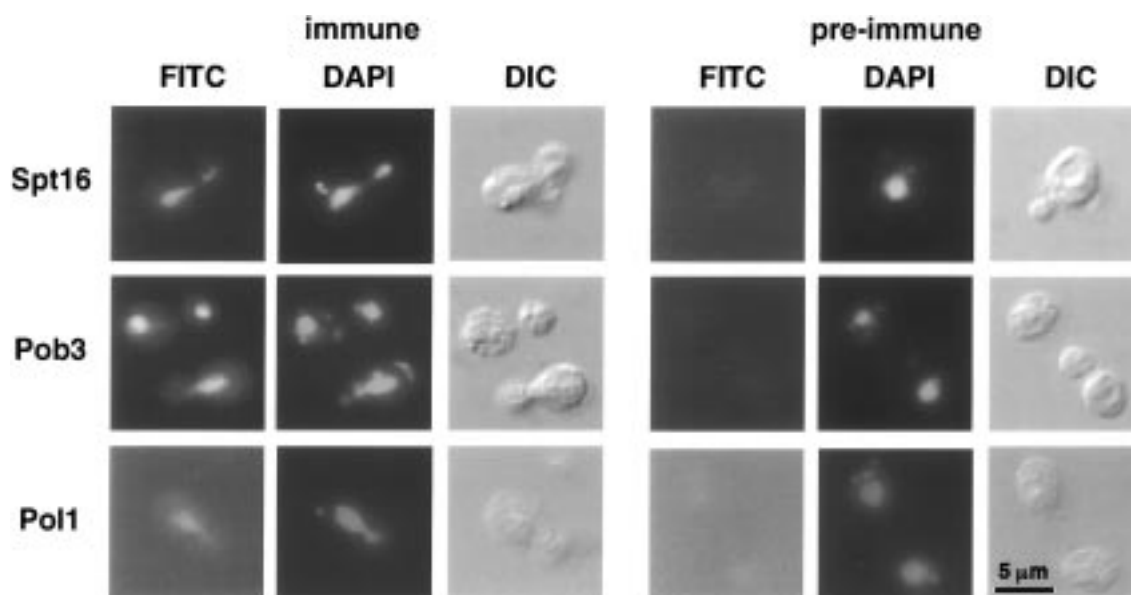


FIGURE 5: Immunolocalization. Spt16, Pob3, and Pol1 were localized to the nucleus by indirect immunofluorescence. The DNA-specific dye DAPI reveals the nucleus and mitochondria. Preimmune and immune refer to the sera from the rabbits before and after injection of the antigens, respectively.

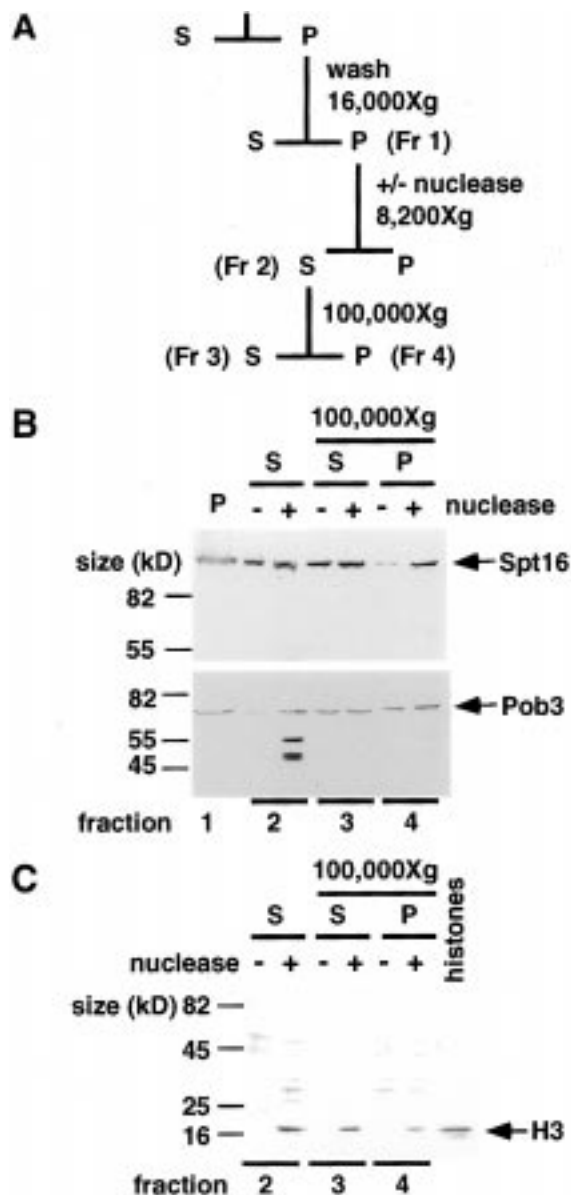


FIGURE 6: Portions of Spt16 and Pob3 fractionate with chromatin. (A) Outline of the chromatin fractionation. (S, supernatants; P, pellets.) Washed, low-speed pellets (fraction 1) from lysed spheroplasts were resuspended in a low ionic strength buffer and incubated in the presence or absence of micrococcal nuclease for 2 min at 37 °C. The nuclease-treated low-speed supernatant (fraction 2) was then centrifuged at 100000g for 1 h. Equal percentages of the high-speed supernatants (fraction 3) and pellets (fraction 4) were separated by SDS–PAGE and either (B) transferred to nitrocellulose and immunoblotted with anti-Spt16 or anti-Pob3 antisera or (C) transferred to nitrocellulose and immunoblotted with anti-histone H3 antiserum. Core histones (3 μ g) purified from chicken erythrocytes were run in an adjacent lane as a positive control.

tion (Figure 6B, fraction 4), consistent with the association of some of the Spt16–Pob3 with chromatin. The amount of Pob3 in the 100000g pellet (fraction 4) may be underestimated because of proteolysis which occurred upon addition of the nuclease (Figure 6B, compare fractions 2 and 4), suggesting either that the nuclease contained a protease or that the release of Pob3 into the supernatant exposed it to a protease which was already present.

To confirm that fraction 4 contained chromatin, the size of DNA molecules and the presence of histone H3 were monitored. Nuclease treatment resulted in the generation of

DNA lengths consistent with a ladder of 1–6 nucleosomes, and the larger members of this population were preferentially pelleted during the high-speed centrifugation (data not shown). Immunodetection revealed that histone H3 was released from fraction 1 by the nuclease (Figure 6B, fraction 2) and was present in both the high-speed centrifugation supernatant and pellet (Figure 6C, fractions 3 and 4). As a negative control, immunodetection of the mitochondrial protein porin in these fractions demonstrated that it was present in the low-speed pellet (fraction 1) and was unaffected by nuclease treatment (data not shown). We conclude that fraction 4 contains chromatin fragments released from the initial insoluble fraction by nuclease digestion that remained large enough to be recovered by high centrifugal forces. A portion of the Spt16 and Pob3 was found in this fraction, indicating that this complex is at least partially associated with chromatin.

The release of Spt16 and Pob3 and the other chromatin components (polynucleosome-length DNA and histone H3) from fraction 1 into the form that was recovered by high-speed centrifugation (fraction 4) was enhanced by, but not completely dependent on, the addition of the nuclease (Figure 6B,C, compare fractions 2 and 4, –/+ nuclease; and data not shown). This may reflect mechanical shearing of the DNA upon resuspension of the low-speed pellet (fraction 1) and/or the activity of endogenous nucleases. Also, since Spt16 and Pob3 distribute between the supernatant and pellet fractions at each step, their association with chromatin is reversible and unstable under the conditions used.

Spt16 and Pob3 Copurify with DNA Polymerase α . The four subunits of the DNA polymerase α complex were overexpressed simultaneously, and the resulting complex was purified. Overexpressed Pol1, Pol12, Pri2, and Pri1 copurified through three chromatographic steps, including anion exchange, hydroxylapatite, and size-exclusion chromatography (Figure 7A), eluting from the latter matrix in the 600 kDa range (Figure 7B).

Immunoblot analysis of individual fractions from size-exclusion chromatography revealed that intact Spt16 and Pob3, as well as an \sim 58 kDa proteolytic fragment of Spt16, coeluted with the Pol α complex (Figure 7C). In some preparations, all of Spt16 was degraded into the \sim 58 kDa fragment at early stages in the Pol α purification and Pob3 was simultaneously lost from the preparation (as in Figure 7A,B; and data not shown). In these cases, the \sim 58 kDa Spt16 fragment still coeluted with the Pol α complex from size-exclusion chromatography, suggesting that this Spt16 fragment is the domain of the Spt16–Pob3 complex responsible for interaction with the Pol α complex.

Three lines of evidence suggest that a minor portion of the total cellular Spt16–Pob3 complex copurified, as opposed to merely coeluted, with the Pol α complex: (1) the majority of the Spt16–Pob3 complex flowed through the phosphocellulose column, whereas a minor portion bound and coeluted with the Pol α complex; (2) the Spt16–Pob3 in association with Pol α eluted at a higher phosphate concentration from the hydroxylapatite column and earlier from the sizing column than Spt16–Pob3 complex alone; and (3) the \sim 58 kDa Spt16 fragment would not be expected to elute from the sizing column in the 600 kDa range if it were not associated with a larger complex. The alteration of

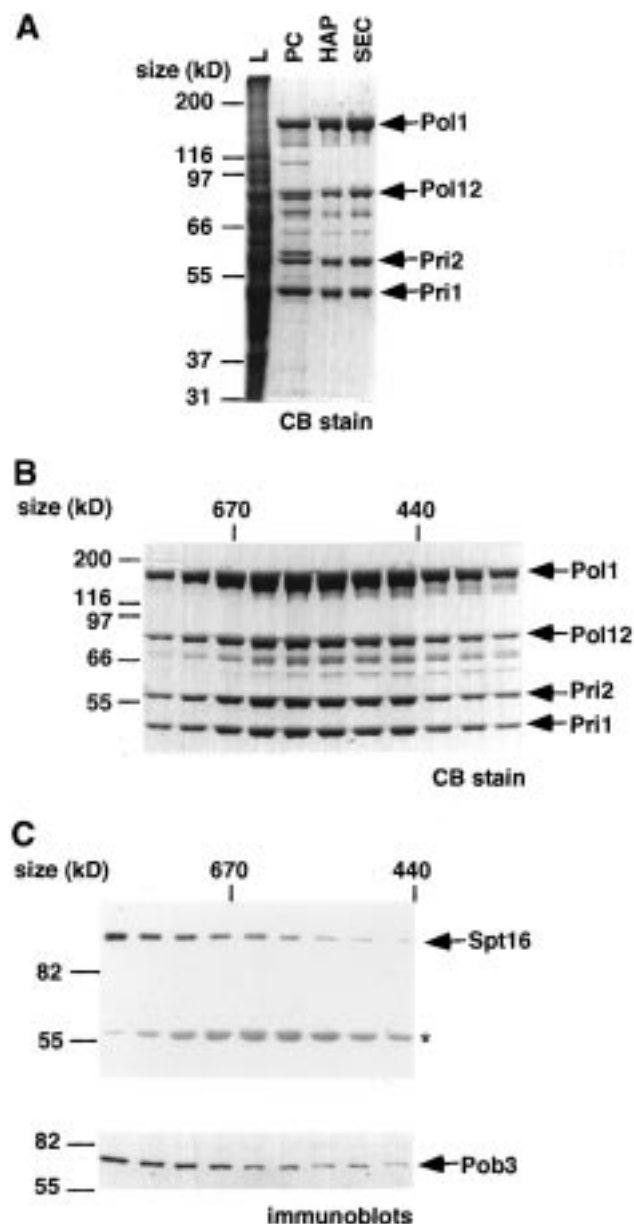


FIGURE 7: DNA polymerase α overexpression and purification. (A) Aliquots of the dialyzed, resuspended ammonium sulfate precipitate from the cell lysate (L) and the eluates from phosphocellulose (PC), hydroxylapatite (HAP), and size-exclusion chromatography (SEC) matrixes were separated by SDS-PAGE and stained with Coomassie blue. Immunoblot analysis revealed that the ladder of minor bands directly below the largest subunit are proteolytic fragments of Pol1 (not shown). Sequencing revealed that the doublet migrating below Pol12 corresponds to two Pol12 proteolytic fragments with NH_2 -termini at residues 116 and 107. The purified Pol α complex was active in the polymerase activity assay previously described (23, and data not shown). (B) Individual fractions from size-exclusion chromatography were separated by SDS-PAGE and stained with Coomassie blue. (C) Immunoblot analysis of individual SEC fractions from a Pol α purification using anti-Spt16 and anti-Pob3 antiserum. In this preparation, both the intact and the degraded forms of Spt16, marked by the asterisk (*), were present, whereas in other preparations, such as the one shown in panels A and B, only the Spt16 fragment (~ 58 kDa) was observed. The molecular masses listed at the top of each panel refer to the standards that were used to calibrate the resin.

the chromatographic properties of this subpopulation of the Spt16-Pob3 complex to correspond with the properties of the Pol α complex indicates that this fraction of Spt16-Pob3 is stably bound to Pol α under a variety of conditions.

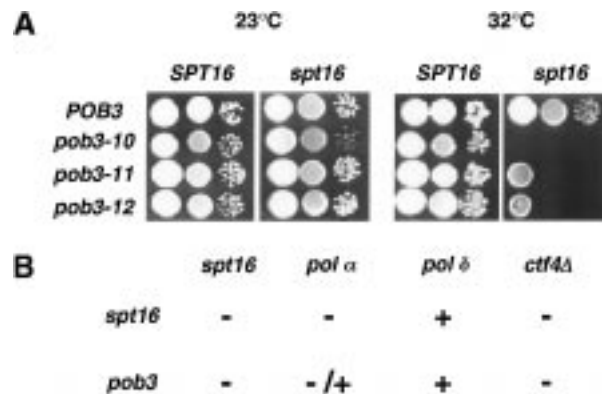


FIGURE 8: Analysis of *spt16* and *pob3* mutants. (A) Strains containing either wild-type or single and double mutant combinations of temperature-sensitive alleles (*spt16*, *pob3-10*, *-11*, *-12*) of *SPT16* and *POB3* were diluted 100-fold serially, spotted onto plates, and incubated at the indicated temperatures for 4 days. All of the *pob3* mutant alleles were present on low-copy (*CEN*) plasmids in *pob3* Δ null strains and are listed under Experimental Procedures as pJW11-x. (B) Schematic representation of the analysis listed in (A) using the *spt16* allele *cdc68-1*, the *pol* α allele *cdc17-1*, the *pol* δ allele *cdc2-1*, and the *pob3* alleles *pob3-10*, *-11*, and *-12*. The (-) and (+) symbols refer to the respective absence or presence of growth at elevated temperatures of cells containing the double mutant combinations listed. The (-/+) refers to the absence of growth when *cdc17-1* was combined with *pob3-10* or *-12*, and the presence of growth when combined with *pob3-11*, respectively.

SPT16 and POB3 Interact Genetically. We mutagenized *POB3* in vitro and used the plasmid shuffle technique to replace a plasmid containing a wild-type *POB3* allele with the mutated versions, and then assayed isolates for conditionally lethal mutations. Three temperature-sensitive alleles were identified.

Since Spt16 and Pob3 interact physically, combining mutations in each gene in the same cell may have a more severe phenotype than each single mutated allele alone. Therefore, we combined temperature-sensitive mutations in *SPT16* and *POB3* and compared the viability of these cells to those containing either single mutant at various temperatures. Combining a temperature-sensitive allele of *SPT16* with any of three temperature-sensitive alleles of *POB3* resulted in decreased viability of cells at temperatures of 30 °C (not shown) or above, with the effect being most dramatic at 32 °C (Figure 8). One likely explanation for this result is that the combination of mutations in *SPT16* and *POB3* destabilizes the complex to a greater extent than either single mutation. This is consistent with our interpretation of the results from size-exclusion chromatography of whole cell lysates that the complex is the functional form of these proteins.

We also observed subtle decreases in viability with combinations of either *pob3-10* or *pob3-12* with a temperature-sensitive allele of *POL1* (*cdc17-1*), between 28 and 31 °C (data not shown), consistent with our previous, and more dramatic, observation with *spt16 pol1* double mutants (3). This suggests that mutations in either *SPT16* or *POB3* affect the interaction of the Spt16-Pob3 complex with Pol1. We did not see an effect on cell viability by combining any of these three *pob3* alleles with a temperature-sensitive allele of the catalytic subunit of DNA polymerase δ (*cdc2-1*, data not shown), demonstrating that this effect does not occur by combining the *pob3* mutations with any polymerase mutation.

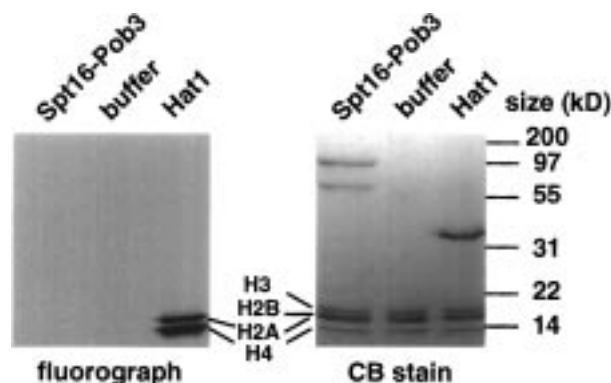


FIGURE 9: Acetyltransferase assay. Purified Spt16–Pob3 complex or Hat1, as a positive control (43, 44), was incubated in a buffer containing [3 H]acetyl-CoA and purified core histones for 30 min at 37 °C. Reactions were quenched by the addition of SDS sample buffer, boiled, separated by SDS–PAGE, stained with Coomassie blue (right panel), and subjected to fluorography (left panel).

Combining any of these three *pob3* alleles with a null mutation in the gene encoding another Pol1-binding protein, *CTF4*, also decreased the viability of the cells at elevated temperatures (data not shown), consistent with our previous observation that an *spt16 ctf4Δ* double mutant is less viable at elevated temperatures relative to either single mutant (3). Spt16 and Pob3 appeared to compete with Ctf4 for binding to Pol1 on an affinity column (3). One explanation for the observed decrease in cell viability in the *pob3 ctf4Δ* and *spt16 ctf4Δ* double mutants is that both the Spt16–Pob3 complex and Ctf4 bind to and stabilize Pol1 at elevated temperatures.

The Spt16–Pob3 Complex Is Not Active in Acetyltransferase or ATPase Assays. Previous genetic analysis implicated *SPT16* as a modulator of chromatin structure, and sequence comparisons revealed a partial match to acetyltransferase motif A (30; and A. Neiman and R. Sternglanz, personal communication). We therefore determined whether the Spt16–Pob3 complex acetylates histones. However, the purified Spt16–Pob3 complex failed to acetylate core histones in an in vitro assay (Figure 9). Furthermore, a triple replacement (Q279A/G282A/G284A) in the conserved acetyltransferase motif A (–Q–X–X–G–X–G–) (30) in Spt16 appears to retain function as it complemented both the temperature-sensitivity of the *spt16* allele *cdc68-1* and an *spt16* null mutant. These replacements lie in a region of Spt16 that shows some similarity to known histone acetyltransferases (HATs) and based on the structure of Hat1 (31), as well as mutagenesis of other HATs (32–37), would likely abolish any acetyltransferase activity in Spt16. It is therefore highly unlikely that histone acetyltransferase activity is involved in the function of Spt16.

The purified Spt16–Pob3 complex, from cells containing either endogenous or overexpressed levels of the complex, did not hydrolyze ATP (data not shown).

DISCUSSION

Spt16 and Pob3 form a stable, abundant, elongated heterodimer that is essential for viability. A portion of the Spt16–Pob3 complex copurified with the DNA polymerase α complex, suggesting that these two complexes form a strong interaction. This is consistent with our previous observations that Spt16 and Pob3 physically interact with

the catalytic subunit of DNA polymerase α , Pol1 (as demonstrated in affinity chromatography and co-immunoprecipitation experiments). The genetic analysis of *SPT16*, *POB3*, and *POL1* suggests that the formation and stability of these complexes are an important feature of the functions of these proteins (Figure 8 and ref 3).

We have also found that Spt16, Pob3, and Pol1 all localize to the nucleus in *S. cerevisiae* and that a portion of the Spt16–Pob3 complex is chromatin-associated. There appear to be at least two populations of Spt16 and Pob3 within the cell: one that forms a stable, soluble heterodimer and another insoluble chromatin-associated pool. The latter pool is not very stably associated with chromatin since some Spt16 and Pob3 was found to be released to a soluble form at each step during the preparation of chromatin. However, some Spt16–Pob3 was solubilized by nuclease treatment to a form that could be recovered by high-speed centrifugation, as expected for chromatin-associated proteins. Indeed, the final high-speed pellet that contained some Spt16 and Pob3 also contained chromatin as assayed by the presence of histones and DNA fragments with the length distribution typical of nucleosomal fragments. We cannot conclude that Spt16–Pob3 binds directly to nucleosomes, but we can conclude that some of this complex cofractionates with chromatin, suggesting it is a component of chromatin.

We failed to detect an in vitro interaction between the purified Spt16–Pob3 complex and histones using the following three techniques: (1) binding to histone agarose (Sigma); (2) binding to GST-fusions of the N-terminal peptides of histones H2A, H2B, H3, and H4; (3) co-immunoprecipitation of the core histones with the Spt16–Pob3 complex using anti-Spt16 antiserum when the purified components were mixed in vitro (data not shown). However, when the purified Spt16–Pob3 complex and the core histones were mixed, the components of both complexes precipitated out of solution under conditions that did not affect the solubility of the components individually. The significance of this, if any, is uncertain.

Analytical ultracentrifugation of the Spt16–Pob3 complex revealed that it is a stable heterodimer. This same stoichiometry was previously suggested for the *S. cerevisiae* complex (25) based on the relative intensity of co-immunoprecipitating tagged and/or mutant versions of Spt16 and Pob3 from silver-stained gels or immunoblots as well as for the *Xenopus* DUF complex based on the intensity of bands in Coomassie blue stained protein bands (11). We find that the more definitive methods of velocity and equilibrium sedimentation of the purified complex firmly establish this stoichiometry. Furthermore, the complex is stable for long periods under a variety of ionic strengths and is the only form of either protein detected in lysates, although we cannot rule out the possibility of an additional, less stably associated subunit.

Our data suggest that this complex, whether purified or from whole cell lysates, runs anomalously in size-exclusion matrixes due to an elongated shape. Both the nonideal behavior in equilibrium sedimentation as well as the axial ratios calculated from the velocity sedimentation experiment are also consistent with the complex having a nonspherical shape. Using the shape factor ($F = f/f_0$) generated from velocity sedimentation of purified Spt16–Pob3, we calculated (assuming a partial specific volume of 0.73 cm³ g^{–1})

that the complex would be 34 nm long \times 2.8 nm wide if it is rod shaped and 16 nm wide \times 1.1 nm high if it is disk shaped. The latter dimensions are unlikely since an average α -helix within a protein is 1–1.5 nm wide, which would require the tertiary fold of a disk-shaped Spt16–Pob3 complex to be a monolayer of secondary protein structure in order to fit into a 1.1 nm space. Furthermore, there is no precedence for a protein with these dimensions and shape. However, there are many examples of proteins with rod-shaped tertiary and quaternary structures (38). If the Spt16–Pob3 complex is rod shaped, then the 2.8 nm width and 34 nm length would have the potential to span more than one nucleosome (11 nm wide).

The *Xenopus* DUF complex elutes from gel filtration chromatography in the size range expected for a heterodimer, suggesting that, unlike yeast Spt16–Pob3, the *Xenopus* complex has a globular shape (11). Pob3 shares 35% identity over its entire length with the DUF87 protein, but lacks the HMG box found in DUF87 and other members of this family, including the mouse T160 and human SSRP proteins (3, 11). A recently identified ortholog of Pob3 from *Schizosaccharomyces pombe* also lacks the HMG box (39). The DNA-binding domain of the mouse T160 protein has been mapped to the HMG box (40). The DNA unwinding activity of the DUF complex (11) and the ability of the mouse T160 (40) and the human SSRP proteins (41) to bind DNA suggest that the HMG box is an important feature of the function of these proteins. The yeast complexes may work without this domain or may act with a less stably associated subunit with DNA-binding activity. The presence or absence of the HMG box within the complex may determine whether the complex adopts a globular or an elongated shape.

Cells containing a temperature-sensitive allele of *SPT16* arrest at the nonpermissive temperature with an unbudded morphology and a 1C DNA content, suggesting that Spt16 functions in the G1 stage of the cell cycle (3, 4). However, the flow cytometry analysis that we used to detect DNA content could not distinguish whether these cells were arrested before, or in the early stages of, S-phase. Therefore, the Spt16–Pob3 complex may still function at the early stages of replication elongation even though the morphological arrest of the *spt16* mutant at the nonpermissive temperature appears to be in G1. Our preliminary analysis using two-dimensional DNA replication intermediate gels (Brewer-Fangmen gels, ref 42) suggests that DNA replication is initiating at the rDNA loci and at ARS305 (an early and efficient firing origin) as demonstrated by the presence of bubble and Y-arcs in the *spt16* mutant strain after 3 h at the nonpermissive temperature of 37 °C (data not shown). Immunodepletion of the DUF complex from *Xenopus* egg extracts severely diminished the ability to replicate exogenously added DNA, strongly suggesting that this complex functions in DNA replication (11).

We favor a model in which the Spt16–Pob3 complex physically interacts with DNA polymerase α to alter the properties of chromatin in the course of DNA replication. This model predicts that Pol α would require the function of the Spt16–Pob3 complex either to access origins of replication in chromatin and/or to allow passage of the replication fork through the nucleosomes that are encountered during elongation.

NOTE ADDED IN PROOF

In a recent publication, Reinberg's group has reported that the previously described human FACT complex (45) is a heterodimer of human homologues of the yeast Spt16 and Pob3 proteins (46). FACT promotes elongation of transcription by RNA polymerase II past nucleosomes on the DNA template that otherwise block progression (45). Our purified yeast Spt16–Pob3 complex did not display FACT activity in the reconstituted human transcription system (D. S. Luse, personal communication), but this could be due to any of several differences between Spt16–Pob3 proteins and their human counterparts, most notably the lack of an HMG1 box in Pob3 (3). The activity of FACT and the similarity of its components with Spt16 and Pob3 proteins provide strong support for the model proposed here that Spt16–Pob3 facilitates assembly or movement of DNA replication complexes on chromatin templates.

ACKNOWLEDGMENT

We thank Greg Hermann, Janet Shaw, and other members of the Shaw lab for assistance with immunofluorescence; Bob Dutnall and Venki Ramakrishnan for the purified core histones and Hat1. We are grateful to Brad Cairns, Dana Carroll, Bob Dutnall, and David Stillman, whose critical comments significantly improved the manuscript.

REFERENCES

1. Kornberg, A., and Baker, T. A. (1992) *DNA Replication*, 2nd ed., W. H. Freeman and Company, New York.
2. Stillman, B. (1994) *Cell* 78, 725–728.
3. Wittmeyer, J., and Formosa, T. (1997) *Mol. Cell. Biol.* 17, 4178–4190.
4. Prendergrast, J. A., Murray, L. E., Rowley, A., Carruthers, D. R., Singers, R. A., and Johnston, G. C. (1990) *Genetics* 124, 81–90.
5. Malone, E. A., Clark, C. D., Chiang, A., and Winston, F. (1991) *Mol. Cell. Biol.* 11, 5710–5717.
6. Lycan, D., Mikesell, G., Bunker, M., and Breeden, L. (1994) *Mol. Cell. Biol.* 14, 7455–7465.
7. Rowley, A., Singer, R. A., and Johnston, G. (1991) *Mol. Cell. Biol.* 11, 5718–5726.
8. Xu, Q., Johnston, G. C., and Singer, R. A. (1993) *Mol. Cell. Biol.* 13, 7553–7565.
9. Xu, Q., Singer, R. A., and Johnston, G. C. (1995) *Mol. Cell. Biol.* 15, 6025–6035.
10. Evans, D. R. H., Brewster, N. K., Xu, Q., Rowley, A., Altheim, B. A., Johnston, G. C., and Singer, R. A. (1998) *Genetics* 150, 1393–1405.
11. Okuhara, K., Ohta, K., Seo, H., Shioda, M., Yamada, T., Tanaka, Y., Dohmae, N., Seyama, Y., Shibata, T., and Murofushi, H. (1999) *Curr. Biol.* 9, 341–350.
12. Formosa, T., and Nittis, T. (1999) *Genetics* 151, 1459–1470.
13. Rose, M. D., Winston, F., and Hieter, P. (1990) *Methods in Yeast Genetics, A Laboratory Course Manual*, Cold Spring Harbor Laboratory Press, Cold Spring Harbor, NY.
14. Hartwell, L. H. (1967) *J. Bacteriol.* 93, 1662–1670.
15. Laemmli, U. K. (1970) *Nature* 227, 680–685.
16. Gietz, R. D., and Sugino, A. (1988) *Gene* 74, 527–534.
17. Chang, Y. C., and Timberlake, W. E. (1992) *Genetics* 133, 29–38.
18. Harlow, E., and Lane, D. (1988) *Antibodies: a laboratory manual*, Cold Spring Harbor Laboratory, Cold Spring Harbor, NY.
19. Johnson, M. L., Correia, J. J., Yphantis, D. A., and Halvorson, H. R. (1981) *Biophys. J.* 36, 575–588.
20. Gill, S. C., and von Hippel, P. H. (1989) *Anal. Biochem.* 182, 319–326.

21. Pringle, J. R., Adams, A. E. M., Drubin, D. G., and Haarer, B. K. (1991) *Methods Enzymol.* 194, 565–602.
22. Liang, C., and Stillman, B. (1997) *Genes Dev.* 11, 3375–3386.
23. Miles, J., and Formosa, T. (1992) *Proc. Natl. Acad. Sci. U.S.A.* 89, 1276–1280.
24. Sikorski, R. S., and Boeke, J. D. (1991) *Methods Enzymol.* 194, 302–318.
25. Brewster, N. K., Johnston, G. C., and Singer, R. A. (1998) *J. Biol. Chem.* 273, 21972–21979.
26. Bouvier, D., and Baldacci, G. (1995) *Mol. Biol. Cell* 6, 1697–1705.
27. Herrick, G., Spear, B. B., and Veomett, G. (1976) *Proc. Natl. Acad. Sci. U.S.A.* 73, 1136–1139.
28. Mizuno, T., Ito, N., Yokoi, M., Kobayashi, A., Tamai, K., Miyazawa, H., and Hanaoka, F. (1998) *Mol. Cell. Biol.* 18, 3552–3562.
29. Nakamura, H., Morita, T., Masaki, S., and Yoshida, S. (1984) *Exp. Cell Res.* 151, 123–133.
30. Neuwald, A. F., and Landsman, D. (1997) *Trends Biochem. Sci.* 22, 154–155.
31. Dutnall, R. N., Tatrov, S. T., Sternglanz, R., and Ramakrishnan, V. (1998) *Cell* 94, 427–438.
32. Tercero, J. C., Riles, L. E., and Wickner, R. B. (1992) *J. Biol. Chem.* 267, 20270–20276.
33. Smith, E. R., Eisen, A., Gu, W., Sattah, M., Pannuti, A., Zhou, J., Cook, R. G., Lucchesi, J. C., and Allis, C. D. (1998) *Proc. Natl. Acad. Sci. U.S.A.* 95, 3561–3565.
34. Lu, L., Berkey, K. A., and Casero, R. A., Jr. (1996) *J. Biol. Chem.* 271, 18920–18924.
35. Kuo, M. H., Brownell, J. E., Sobel, R. E., Ranalli, T. A., Cook, R. G., Edmonson, D. G., Roth, S. Y., and Allis, C. D. (1996) *Nature* 383, 269–272.
36. Hilfiker, A., Hilfiker-Kleiner, D., Pannuti, A., and Lucchesi, J. C. (1997) *EMBO J.* 16, 2054–2060.
37. Coleman, C. S., Huang, H., and Pegg, A. E. (1996) *Biochem. J.* 316, 697–701.
38. Creighton, T. E. (1993) *Proteins: Structures and Molecular Properties*, 2nd ed., W. H. Freeman and Company, New York.
39. Altschul, S. F., Madden, T. L., Schaffer, A. A., Zhang, J., Zhang, Z., Miller, W., and Lipman, D. J. (1997) *Nucleic Acids Res.* 25, 3389–402.
40. Shirakata, M., Huppi, K., Usuda, S., Okazaki, K., Yoshida, K., and Sakano, H. (1991) *Mol. Cell. Biol.* 11, 4528–4536.
41. Bruhn, S. L., Pil, P. M., Essigmann, J. M., Housman, D. E., and Lippard, S. J. (1992) *Proc. Natl. Acad. Sci. U.S.A.* 89, 2307–2311.
42. Friedman, K. L., and Brewer, B. J. (1995) *Methods Enzymol.* 262, 613–627.
43. Kleff, S., Andrusis, E. D., Anderson, C. W., and Sternglanz, R. (1995) *J. Biol. Chem.* 270, 24674–24677.
44. Parthun, M. R., Widom, J., and Gottschling, D. E. (1986) *Cell* 87, 85–94.
45. Orphanides, G., LeRoy, G., Chang, C.-H., Luse, D. S., and Reinberg, D. (1998) *Cell* 92, 105–116.
46. Orphanides, G., Wu, W.-H., Lane, W. S., Hampsey, M., and Reinberg, D. (1999) *Nature* (in press).

BI982851D